

Enhanced Crack Width and Depth Measurement through Binary Image Processing and Geometric Analysis

Kavita Bodke^{1,A}, Sunil Bhirud^{2,B}, Keshav Kashinath Sangle^{3,A}

^A Veermata Jijabai Technological Institute, Mumbai, India

^B COEP Technological University, Pune, India

¹ ORCID: 0000-0003-4498-5393, kvbodke_p21@ce.vjti.ac.in

² ORCID: 0000-0002-9100-6437

³ ORCID: 0000-0003-0618-7526

Abstract

This paper presents a novel, image-based approach for automatically quantifying structural crack width and depth in concrete using binary image processing techniques. Concrete cracks are critical indicators of potential structural failure, and traditional manual inspection methods are often time-consuming, unsafe, and prone to inaccuracies. The proposed method automates crack detection by converting RGB images of concrete surfaces into binary images, isolating the cracks, and measuring their width using the Euclidean distance formula. The depth of the cracks is then estimated using trigonometric relationships based on the measured crack width and viewing angles (30°, 45°, and 60°). This lightweight, cost-effective approach provides a practical alternative to more complex machine learning-based detection methods, making it ideal for real-time infrastructure health monitoring. The results highlight the effectiveness of this technique in accurately measuring crack width and depth across multiple angles, providing critical data for infrastructure health monitoring.

Keywords: Crack width, crack depth, Euclidean distance, binary image processing, trigonometry, structural health monitoring.

Introduction

Crack detection in materials, especially in infrastructure such as roads, bridges, and buildings, is critical for ensuring structural integrity and public safety. Over time, various environmental factors, including weathering and load stress, can cause cracks that, if left unchecked, may lead to structural failure. Traditional crack detection methods rely heavily on manual inspection, which is time-consuming, subjective, and often prone to human error.

Recent advancements in image processing and machine learning have opened new avenues for automating crack detection. Convolutional neural networks (CNNs), a type of deep learning architecture, have proven particularly effective in analyzing visual data for tasks like object recognition, segmentation, and defect detection. By leveraging CNNs, automated crack detection systems can provide faster, more accurate assessments of surface damage. However, these methods often require substantial computational resources and may be difficult to implement in real-time monitoring systems. In contrast, simpler approaches such as binary image processing provide a cost-effective and efficient solution for crack measurement, making them more practical for field applications.

Historically, crack detection and measurement have relied on manual methods such as visual inspections, calipers, or rulers. While these approaches may be straightforward, they are labor-intensive, time-consuming, and prone to human error. Furthermore, manual inspections are not suitable for regular, long-term monitoring, making it difficult to track crack

propagation over time. As a result, the need for automated, precise, and efficient crack detection methods has led to a growing interest in image processing techniques.

This research aims to develop an image-based crack quantification that can measure crack width and estimate crack depth. By employing noise reduction techniques and calculating crack depth using geometric properties such as angles and width, the system can provide a comprehensive analysis of cracks. The proposed method offers a more objective and scalable solution than traditional approaches, potentially improving the accuracy and efficiency of crack detection in various applications.

Related work

1. Crack Detection Using Image Processing

Crack detection is a critical component of structural health monitoring (SHM), and various image-processing techniques have been proposed to automate this process. One of the most recent approaches involves convolutional neural networks (CNNs), which have shown considerable success in automating crack detection. Omar et al. (2018) introduced a CNN-based method for detecting cracks in concrete structures. Their work demonstrated that deep learning could significantly improve detection accuracy compared to traditional edge detection and thresholding techniques. Similarly, Zou et al. (2019) developed **DeepCrack**, a CNN model designed to learn hierarchical convolutional features, resulting in precise crack detection in various environments. These machine learning methods, while highly accurate, require significant computational resources and extensive training data, which may limit their practicality in real-time or low-resource environments.

Other researchers have explored more traditional image processing methods. Yamaguchi and Hashimoto (2010) proposed a fast crack detection algorithm for processing large concrete surface images using percolation-based techniques. This grayscale-based method focuses on the rapid analysis of large-scale images, making it well-suited for field applications where high-resolution images are involved. However, the grayscale approach may struggle with complex surfaces or lighting variations.

How it relates to our work: Our approach differs by focusing on binary image processing, which provides a lightweight and computationally efficient alternative to complex machine learning techniques. Instead of requiring extensive datasets for training, we apply simple thresholding and geometric analysis, making our method more accessible for real-time monitoring and scalable to large datasets without significant computational overhead.

2. Crack Depth Measurement Techniques

While crack detection has been widely studied, fewer works have focused on the accurate measurement of crack depth. Hutchinson and Chen (2006) explored the use of image analysis to estimate crack dimensions, including width and depth, as part of concrete damage evaluation. Their approach combined image analysis with manual depth measurements, highlighting the challenges of obtaining precise depth information from 2D images.

Li et al. (2018) took this a step further by using stereo imaging to measure crack depth in civil engineering applications. By capturing images from slightly different angles, they were able to create a 3D depth map, providing a more detailed understanding of crack propagation beneath the surface. However, stereo imaging requires specialized equipment and image processing capabilities, which may not be feasible for many monitoring scenarios.

Another approach is digital image correlation (DIC), which Liu and Sun (2017) applied to quantify crack depth and width in concrete structures. DIC techniques rely on deformation patterns to measure surface displacement and infer crack dimensions, providing high accuracy but requiring sophisticated setups.

How it relates to our work: Our method offers a simpler, cost-effective alternative to stereo imaging and DIC by estimating crack depth based on the Euclidean distance between pixel coordinates in a binary image. Using geometric relationships and trigonometric calculations, we derive depth information from 2D images without the need for advanced 3D recon-

struction or specialized hardware. This approach is particularly valuable for routine, large-scale monitoring where resource efficiency is critical.

3. Euclidean Distance in Image Processing

The Euclidean distance formula is a fundamental tool in image processing, frequently used for measuring distances between features in an image. Duda and Hart (1972) introduced the use of geometric relationships such as Euclidean distance in early edge detection algorithms. This foundational concept has since been applied in a variety of contexts, including crack measurement. Wang et al. (2019) used the Euclidean distance between the edges of detected cracks to calculate crack width in concrete surfaces. Their approach combines adaptive Gaussian fitting with distance measurement, producing highly accurate width estimates in real-world scenarios.

How it relates to our work: In our research, we build on the traditional use of Euclidean distance by applying it specifically to measure crack width in binary images. By calculating the distance between the first and last detected white pixels in each row, we determine the crack's width. This simple, direct approach is well-suited for our goal of calculating both width and depth using lightweight image processing techniques.

4. Thresholding and Binary Image Analysis

Thresholding is one of the most widely used techniques in image processing for converting grayscale images to binary images, where objects of interest can be isolated. Otsu (1979) proposed a method for selecting an optimal threshold based on gray-level histograms, which has since become a standard in image segmentation tasks. Sahoo et al. (1988) provided a comprehensive review of various thresholding methods, including global, local, and adaptive techniques, that apply to a wide range of image analysis tasks.

Binary image processing, as a result of thresholding, is often the first step in object detection, edge detection, and feature extraction in images. It allows for the simplification of complex images by reducing them to two colors—typically black and white—representing the background and the object of interest, respectively.

How it relates to our work: We employ binary thresholding to isolate cracks from the rest of the image, converting the input RGB image into a format that simplifies the analysis. This method allows us to detect white pixels representing cracks, providing the foundation for subsequent width and depth calculations. While our method builds on traditional binary segmentation techniques, it extends these methods by using geometric functions to estimate crack depth, which is a novel contribution.

5. Applications in Structural Health Monitoring

Structural health monitoring (SHM) has increasingly relied on image-based techniques for assessing infrastructure integrity. Choi and Shah (1997) discussed how image analysis can be used to measure deformations in concrete specimens, highlighting its applicability in crack growth monitoring. More recently, Zhang et al. (2020) proposed a vision-based approach for automatic crack detection and quantification, contributing to the development of non-destructive testing (NDT) methods for civil engineering.

Image-based SHM methods offer the advantage of being non-invasive, allowing for the continuous monitoring of critical structures such as bridges, tunnels, and buildings without the need for direct physical access. This has significant implications for safety and maintenance, as early detection of cracks can prevent catastrophic failure and extend the life of critical infrastructure.

How it relates to our work: Our research contributes to the growing field of image-based SHM by offering a method for detecting and quantifying cracks without the need for expensive or complex equipment. The ability to measure crack width and depth using simple image processing techniques makes our approach a viable tool for real-time infrastructure monitoring, especially in scenarios where cost and computational resources are limited.

Contribution

Several studies have explored fracture detection approaches and algorithms, but few have focused on crack width assessment, which is crucial for safety diagnosis.

We describe a crack detection technique that improves in detecting crack width and depth, an important aspect of safety inspection. The suggested technique involves steps: converting the image into a binary image, thresholding, detecting cracks, detecting distance (width) using the Euclidean distance formula, and finally depth calculation using a simple trigonometric formula. Its key advantage is more precise fracture pixel extraction. This method helps analyze the depth of cracks in an image by identifying colored pixels, calculating the distance between them, and converting this distance into a real-world depth measurement.

In computer vision, effective image processing techniques are essential for extracting meaningful information from visual data. Figure 1 shows a flow diagram of a systematic approach to processing an input image, leveraging Python libraries such as OpenCV and pandas.

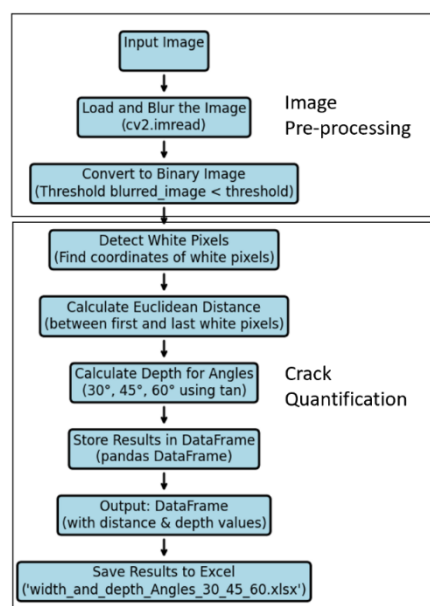


Figure 1. Flow Diagram

In the first step, in the preprocessing phase, Gaussian blur was applied to the original image to reduce noise and enhance the clarity of the features relevant to crack detection. The Gaussian blur operates by convolving the image with a Gaussian kernel, effectively smoothing the image and diminishing high-frequency noise that could interfere with accurate analysis. This step is crucial, as it ensures that the subsequent binary thresholding operation is performed on a cleaner image, thereby improving the reliability of the crack detection process.

The second step, in the crack quantification process, involves converting a blurred image of a cracked surface into a binary (black-and-white) image. This transformation simplifies the analysis by reducing the complexity of the data, allowing the cracks to be easily distinguished from the background.

The conversion is achieved through **thresholding**, where a threshold level is applied to the blurred channels of the image. In this work, a threshold level of 4 is set, meaning that any pixel with blurred image values less than 4 is classified as a white pixel (representing the crack), while all other pixels are classified as black (representing the background). This process is performed using the following condition for each pixel:

$$Pixel_{binary} = \begin{cases} 255 & \text{if } blurred_{pixel} < 4 \\ 0 & \text{otherwise} \end{cases} \quad (1)$$

The output is a binary image with white pixels representing cracks (value 255) and a black background (value 0). This step isolates the crack features from the surrounding material, enabling subsequent measurements of crack width and depth.

A. Crack Quantification Methodology

Crack quantification is essential in various fields, such as structural health monitoring, material science, and civil engineering, where precise measurements of crack dimensions are crucial for assessing damage, understanding material behavior, and predicting failure. This research employs an image-based method to measure crack width and depth from digital images using image processing techniques.

In this research, crack quantification is performed using image processing techniques to measure both the width and the depth of cracks in a given image. The approach involves transforming an RGB image of a cracked surface into a binary image and applying spatial measurements to quantify the crack's geometric characteristics. Below is a detailed description of the approach used for crack quantification.

Figure 2 shows the actual image converted into a blur image for noise reduction. We used Gaussian Blur for noise reduction, and adjusted kernel size as we needed.

Image is captured by camera resolution $1800 * 4000$ pixels (Width * height) with 72 DPI for both horizontal and vertical resolution.

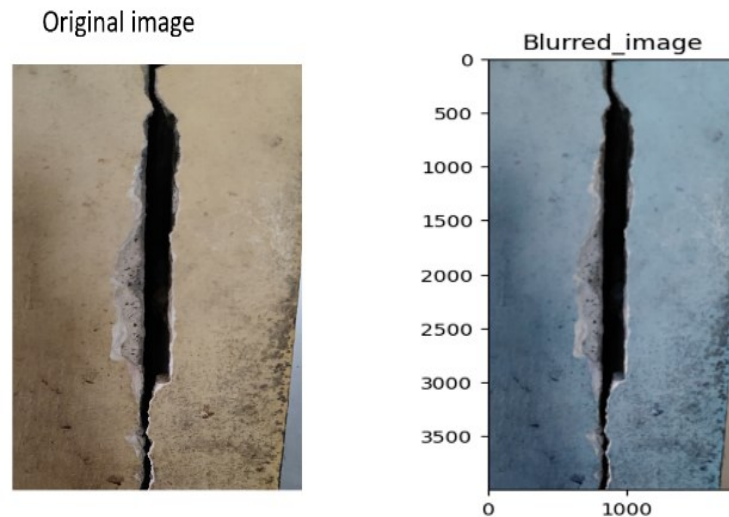


Figure 2 Actual image vs blurred image

B. Methodology for Width Calculation

Crack width is defined as the linear measurement of the gap or fissure at its widest point. It is a crucial parameter in evaluating the severity of cracks, as wider cracks often indicate more significant structural distress.

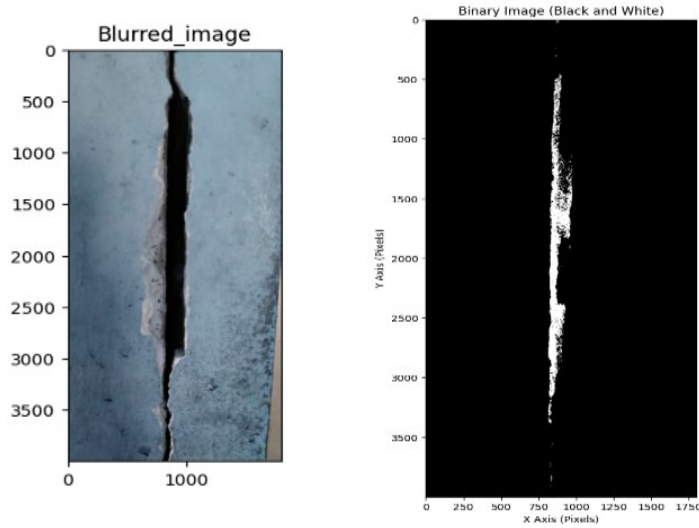


Figure 3 binary image for width calculation

Figure 3 shows the blurred image converted into a binary image for width calculation. We analyze the binary image row by row to quantify the crack width. For each row, the algorithm identifies the positions of the first and last white pixels, which correspond to the edges of the crack. The Euclidean distance between these points is calculated to determine the crack width by using the below formula: -

$$D = \sqrt{(x_2 - x_1)^2 + (y_2 - y_1)^2} \quad (2)$$

where (x_1, y_1) and (x_2, y_2) are the coordinates of the first and last white pixels, respectively. In a horizontal row, this simplifies to:

$$D = |\text{Last white pixel} - \text{First white pixel}| \quad (3)$$

The scaler factor depends on the dot per inch (DPI) or pixel per inch (PPI). Higher PPI and DPI indicate higher clarity and quality of the image. In this research, we used DIP resolution for images. The pixel-to-mm conversion is mostly used for real-world data, the formula for pixel-to-mm is as follows:

$$mm = (\text{pixel} * 25.4) / \text{DPI or PPI} \quad (4)$$

The calculated distance in pixels is converted to millimeters using the same scale factor S:

$$D_{mm} = D_{\text{pixel}} * S \quad (5)$$

D_{mm} : distance in mm

D_{pixel} : distance in pixel

$$S = \frac{25.4}{72 (\text{DPI})} \quad (6)$$

For this paper scale factor is equal to 0.3527mm. The final formula conversion of pixel to mm for this paper is:

$$D_{mm} = D_{\text{pixel}} * 0.3527 \quad (7)$$

As shown in **Figure 7**, manual ruler measurements were used to validate the pixel-to-millimeter conversion factor. The observed difference between physical and automated measurements was typically within ± 0.1 mm, which we take as the first-order approximation of the conversion error.

Threshold and Scale Factor Selection

- **Threshold Selection:** In the initial demonstration, a fixed threshold value of 4 was used for binarization to illustrate the crack extraction process on a specific image. However, for subsequent experiments and validation, Otsu's automatic thresholding method was employed. This approach determines the optimal threshold dynamically from the grayscale histogram of each image, ensuring robust separation of cracks from the background under different lighting and surface conditions. The use of an adaptive threshold improves reproducibility when applying the method to other datasets and shooting environments.

- **Scale Factor Calibration:** The scale factor of 0.3527 mm/pixel in this study was determined by relating the physical size of the specimen surface (10 cm × 20 cm) to the captured image resolution (1800 × 4000 pixels). This calibration allows pixel-based distances to be expressed in millimeters. For other imaging setups, the scale factor may vary depending on camera resolution, field of view, and the distance between the camera and specimen. To ensure reproducibility across different conditions, the scale factor can be recalibrated by including a reference object of known dimensions within the captured image.

C. Methodology for Depth Calculation

Crack depth refers to the measurement from the surface of a material down to the deepest point of the crack. Understanding crack depth is vital for evaluating the potential for further structural failure. Crack width was calculated based on the Euclidean distance between each row's first and last white pixels, factoring in the angle of interest. Depth Calculation at Specified Angles: The depth of the crack at specific angles (30°, 45°, and 60°) is computed using trigonometric relationships. The depth d at angle θ can be expressed as:

$$\text{Depth} = D * \tan(\theta) \quad (8)$$

The above formula is the original trigonometry formula for depth detection used. We modify this as follows:-

$$D = Dmm / 2 * \tan(\theta) \quad (9)$$

- Depth at 30°:

$$D_{30} = Dmm / 2 * \tan(30) \quad (10)$$

- Depth at 45°:

$$D_{45} = Dmm / 2 * \tan(45) \quad (11)$$

- Depth at 60°:

$$D_{60} = Dmm/2 * \tan(60) \quad (12)$$

Depth-to-Width Ratio Table

The depth-to-width ratio at various angles provides a comparative view of how the depth changes relative to the crack width. This data is useful for understanding how angle variations affect the depth estimate for a given width. Table 1 demonstrates that:

- At **30°**, the depth is approximately 57.7% of the width.
- At **45°**, the depth value is half of the width.
- At **60°**, the depth is significantly greater, at 173.2% of the width.

Table 1 Ratio table

Angle (θ)	Depth-to-Width Ratio	Example (10 mm width)	Estimated Error*
30°	0.577	2.88 mm	±0.55 mm (≈19%)
45°	1	5.00 mm	±0.90 mm (≈18%)
60°	1.732	8.66 mm	±1.70 mm (≈20%)

D. Visual representation of crack quantification technique

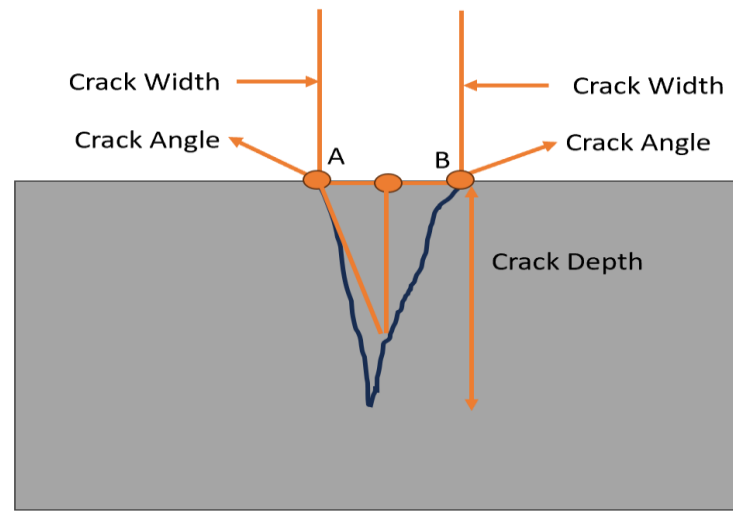


Figure 4. Visual representation of crack

Figure 4, illustrates the geometric relationships between **crack width**, **crack depth**, and **crack angle** in a structural material, such as concrete.

The horizontal distance between points **A** and **B** at the surface of the material. The **Crack Width** is the horizontal distance between points A and B, and the **Crack Angle** is the angle formed by the surface and the sides of the crack at those points. It represents how much the material has separated horizontally due to the crack. This is one of the critical parameters in crack analysis because it helps to quantify the extent of damage at the surface level. In real-world analysis, this crack width is measured in millimeters (mm) using techniques such as image analysis or direct measurement.

The vertical distance from the material's surface down to the crack's deepest point. This parameter is essential because it determines how deep the crack has penetrated the material, which directly affects the component's structural integrity. Deeper cracks pose a greater risk to the stability of the structure. Crack depth is usually estimated using trigonometric relationships between the width and the angle of the crack, or by non-destructive testing techniques such as ultrasonic testing or radiography. The angle formed between the surface of the material and the sides of the crack, at points **A** and **B**. The crack angle helps to estimate the **depth** of the crack using trigonometry. For example, the steeper the crack angle (closer to 90°), the deeper the crack for a given width. Typical crack analysis involves assuming a fixed crack angle (such as 45°) or measuring it through detailed inspection or modeling.

Points A and B are at the edges of the crack where the separation begins at the surface. From these points, the crack extends downward into the material, forming a triangular shape. By measuring the **crack width** and knowing the **crack angle**, the depth of the crack can be calculated using trigonometric relationships. For example, assuming a 30° angle, the depth (h) can be approximated by using the formula:

$$Depth = \frac{Crack\ width}{2} \times \tan(30) \quad (13)$$

The wider the crack and the steeper the angle, the deeper the crack will extend into the material. **Crack Width** and **Crack Depth** are crucial indicators for assessing the severity of cracks in structures. Wider and deeper cracks may indicate more severe damage, requiring immediate attention. **Crack Angle** affects the way forces are distributed across the crack and determines the depth of the crack to its width.

This formula 13 assumes symmetrical angles (the same on both sides) and horizontal distance to the **adjacent** side in a right triangle (known as **tangent** function). If the angles are different at A and B, then you would need to calculate the depth for each side separately and add them:

For side A:

$$Depth_A = \frac{Crack\ width}{2} \times \tan(crack\ angle\ at\ A)$$

For side B:

$$Depth_B = \frac{Crack\ width}{2} \times \tan(crack\ angle\ at\ B)$$

Finally, sum the depths from both sides of the crack angles at A and B are different:

$$Total\ depth = Depth_A + Depth_B$$

Experimental results

This section presents the experimental results of the crack width and depth measurements obtained through image processing techniques, including binary thresholding and Euclidean distance calculations. The results are displayed in both tabular and graphical formats, followed by a discussion that interprets the findings, highlights their significance, and compares them with previous research.

Table 2 Result

Row	Euclidean Distance (mm)	Depth @ 30° (mm)	Depth @ 45° (mm)	Depth @ 60° (mm)
0	9.525	2.749631	4.7625	8.248892
1	9.525	2.749631	4.7625	8.248892
2	10.23056	2.953307	5.115278	8.859921
3	5.997222	1.731249	2.998611	5.193747
4	6.35	1.833087	3.175	5.499261
5	6.35	1.833087	3.175	5.499261
6	5.644444	1.629411	2.822222	4.888232
7	4.938889	1.425734	2.469444	4.277203
8	4.233333	1.222058	2.116667	3.666174
9	6.35	1.833087	3.175	5.499261

A. Crack Width and Depth Measurements

Table 2 and Figure 5 provide the measured **crack width** and corresponding **depth estimates** for cracks detected in a concrete structure. The values are extracted from an image analysis, where each row in the table represents the measurement data for cracks detected in consecutive rows of the image. The data set comprises 10 samples, each showing how the calculated crack depth varies as a function of the crack angle and the Euclidean distance.

The results highlight the variability of crack width and depth across different rows and demonstrate the impact of measurement angles on crack depth estimation.

The Euclidean Distance for each sample, the Euclidean distance remains relatively consistent with some variation across the samples. It ranges between approximately 5 mm and 15 mm.

Depth @ 30°, This column represents the estimated crack depth when viewed at an angle of 30 degrees. Depth is derived from the width using trigonometric principles. For instance, in row 0, the estimated depth at 30° is **2.749631 mm**. In row 3, the depth is **1.731249 mm**.

Depth @ 45°, This column lists the estimated depth of the crack when viewed at a 45-degree angle. The depth increases compared to the 30° estimate, reflecting the trigonometric relationship between viewing angle and depth. For example, Row 0 has a depth of **4.7625 mm** at 45°. Row 3 shows a depth of **2.998611 mm** at 45°.

Depth @ 60°, This column provides the estimated depth when viewed at an angle of 60 degrees, which generally shows the highest depth value due to the steeper angle, suggesting that greater angles tend to exaggerate the perceived crack depth. For example, in row 0, the estimated depth at 60° is **8.248892 mm**. In row 3, the estimated depth is **5.193747 mm**.

Impact of angle on crack depth the crack depth increases significantly as the angle increases from 30° to 60°. This is consistent with the geometric expectation that higher angles inflate

depth readings. The Euclidean distance remains a stable metric, unaffected by changes in the angle, and provides a consistent reference for evaluating true crack lengths.

This serves as an essential part of crack analysis, providing precise measurements of crack width and depth. These measurements contribute to the overall assessment of structural health, allowing for more effective monitoring and maintenance of concrete structures. The use of multiple viewing angles enhances the accuracy and reliability of the depth estimates, making it a valuable tool for engineers and researchers in the field of structural health monitoring.

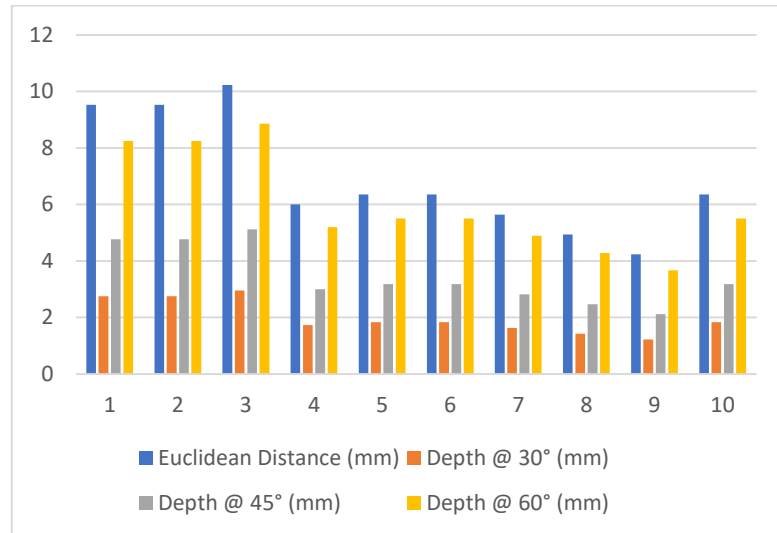


Figure 5 Bar chart

B. Validation with Manual Measurements

To further evaluate the accuracy of the proposed approach, additional validation experiments were performed on a concrete specimen where both physical and image-based crack width measurements were available. Manual crack widths were recorded at marked intervals using a ruler, while the same crack was analyzed using the proposed image-based method.

Figure 3 shows an annotated image of the crack where manual measurements (in cm) are written beside the specimen, and the corresponding automated results (in mm) are superimposed in red. The comparison demonstrates close agreement: for example, a manual measurement of 0.3 cm corresponds to an automated result of approximately 3 mm, while 0.5 cm corresponds to 5 mm.

To further confirm calibration accuracy, a physical scale was placed directly across the crack, as shown in Figure 6. This reference measurement illustrates how the pixel-to-millimeter conversion factor was derived and validated. Using the physical scale, the error between manual and automated measurements was estimated to be within ± 0.2 mm for crack width. Table 3 presents selected comparison results, highlighting the consistency between manual and automated measurements.



Figure 6 Crack width validation: manual measurements (cm) versus automated results (mm)

These results confirm that the proposed method produces measurements consistent with independent manual readings, thereby reinforcing its accuracy and reliability. While the validation was performed on a specimen different from that used in the main experiments, it provides strong supporting evidence of the method's robustness.



Figure 7 Manual measurement of crack width using a physical ruler (scale in centimeters) for calibration and validation of the pixel-to-millimeter conversion factor.

Table 3. Comparison of manual and automated crack width measurements

Location	Manual Measurement (cm)	Manual Equivalent (mm)	Automated Measurement (mm)	Difference (mm)
Point 1	0.2 cm	2 mm	1 mm	1
Point 2	0.3 cm	3 mm	3 mm	0
Point 3	0.3 cm	3 mm	3 mm	0
Point 4	0.3 cm	3 mm	3 mm	0
Point 5	0.3 cm	3 mm	3 mm	0
Point 6	0.3 cm	3 mm	3 mm	0
Point 7	0.3 cm	3 mm	3 mm	0
Point 8	0.4 cm	4 mm	4 mm	0

Point 9	0.5 cm	5 mm	5 mm	0
---------	--------	------	------	---

C. Error Estimation (First Approximation)

Although the proposed method demonstrates good agreement with manual crack width measurements, it is also important to evaluate potential error sources. In this study, two main sources of uncertainty are considered: (A) the conversion from pixels to millimetres and (B) the assumption of a uniform crack slope (30° , 45° , 60°) for depth estimation.

A. Pixel-to-Millimetre Conversion Error

The scale factor used in this study (e.g., 0.0909 mm/pixel, calibrated from the ruler in 7) converts pixel distances into real-world units. Small errors in calibration or pixel localization propagate into width measurement errors. For a measured crack width of 5 mm, the propagated width error is approximately ± 0.1 mm ($\approx 2\%$).

B. Depth Estimation Error

Crack depth is derived from formula 9. Any uncertainty in measured width and assumed slope propagates to depth error. Because the tangent function amplifies slope variations, even a $\pm 5^\circ$ variation in the assumed crack angle can lead to $\sim 18\text{--}20\%$ relative error in depth estimation, whereas width error contributes only $\sim 1\%$.

Future Work

The methodology can be adapted for various use cases, including assessing structural damage in buildings, evaluating surface cracks in materials, and monitoring the integrity of infrastructure. Future work may include enhancing the algorithm to detect and quantify more complex crack patterns, such as branching cracks or cracks with irregular edges. Additionally, integrating machine learning techniques could further automate the process and improve accuracy in identifying and classifying different types of cracks.

This crack quantification method provides a systematic approach for measuring crack width and depth using image processing techniques, enabling detailed analysis of crack characteristics for research and practical applications in material science and engineering.

References

1. Choi, S., & Shah, S. P. (1997). Measurement of deformations on concrete specimens using image analysis. *Experimental Mechanics*, 37(3), 272–278. <https://doi.org/10.1007/BF02317417>
2. Duda, R. O., & Hart, P. E. (1972). Use of the Hough transformation to detect lines and curves in pictures. *Communications of the ACM*, 15(1), 11–15. <https://doi.org/10.1145/361237.361242>
3. Hutchinson, T. C., & Chen, Z. (2006). Improved image analysis for evaluating concrete damage. *Journal of Computing in Civil Engineering*, 20(3), 210–216. [https://doi.org/10.1061/\(ASCE\)0887-3801\(2006\)20:3\(210\)](https://doi.org/10.1061/(ASCE)0887-3801(2006)20:3(210))
4. Li, Z., Yu, X., & He, W. (2018). Three-dimensional crack depth measurement for civil engineering applications using stereo imaging. *Sensors*, 18(3), 839. <https://doi.org/10.3390/s18030839>
5. Liu, S., & Sun, L. (2017). Application of digital image correlation for crack detection and quantification in concrete structures. *Advances in Civil Engineering*, 2017, Article ID 8023680. <https://doi.org/10.1155/2017/8023680>
6. Omar, M., El-Basyouny, N., Khat tab, A., & El-Gizawy, M. (2018). Image-based crack detection in concrete structures using convolutional neural networks. *Automation in Construction*, 91, 116–130. <https://doi.org/10.1016/j.autcon.2018.03.005>
7. Otsu, N. (1979). A threshold selection method from gray-level histograms. *IEEE Transactions on Systems, Man, and Cybernetics*, 9(1), 62–66. <https://doi.org/10.1109/TSMC.1979.4310076>

8. Sahoo, P. K., Soltani, S., & Wong, A. K. C. (1988). A survey of thresholding techniques. *Computer Vision, Graphics, and Image Processing*, 41(2), 233–260. [https://doi.org/10.1016/0734-189X\(88\)90022-9](https://doi.org/10.1016/0734-189X(88)90022-9)
9. Wang, X., Yang, Q., Wang, J., & Li, X. (2019). Crack width measurement based on image processing and adaptive Gaussian fitting. *Measurement*, 148, 106877. <https://doi.org/10.1016/j.measurement.2019.106877>
10. Yamaguchi, T., & Hashimoto, S. (2010). Fast crack detection method for large-size concrete surface images using percolation-based image processing. *Machine Vision and Applications*, 21(5), 797–809. <https://doi.org/10.1007/s00138-009-0199-8>
11. Zhang, Z., Li, Q., Mao, Z., & Shi, Z. (2020). A vision-based approach for automatic crack detection and quantification in concrete structures. *Construction and Building Materials*, 251, 118965. <https://doi.org/10.1016/j.conbuildmat.2020.118965>
12. Zou, Q., Zhang, L., Li, Q., Qi, X., Wang, Q., & Wang, S. (2019). DeepCrack: Learning hierarchical convolutional features for crack detection. *IEEE Transactions on Image Processing*, 28(3), 1498–1512. <https://doi.org/10.1109/TIP.2018.2878966>